J|A|C|S ARTICLES

Published on Web 02/16/2010

Probing Substituent Effects in Aryl−Aryl Interactions Using Stereoselective Diels−Alder Cycloadditions

Steven E. Wheeler,[†] Anne J. McNeil,[‡,§] Peter Müller,[‡] Timothy M. Swager,*[,‡] and K. N. Houk*[,†]

Department of Chemistry and Biochemistry, University of California, Los Angeles, California 90095, and Department of Chemistry, Massachusetts Institute of Technology, Cambridge, Massachusetts 02139

Received May 5, 2009; E-mail: tswager@mit.edu; houk@chem.ucla.edu

Abstract: Stereoselective Diels−Alder cycloadditions that probe substituent effects in aryl−aryl sandwich complexes were studied experimentally and theoretically. Computations on model systems demonstrate that the stereoselectivity in these reactions is mediated by differential π-stacking interactions in competing transition states. This allows relative stacking free energies of substituted and unsubstituted sandwich complexes to be derived from measured product distributions. In contrast to gas-phase computations, dispersion effects do not appear to play a significant role in the substituent effects, in accord with previous experiments. The experimental π-stacking free energies are shown to correlate well with Hammett σ_m constants ($r = 0.96$). These substituent constants primarily provide a measure of the inductive electron-donating and -withdrawing character of the substituents, not donation into or out of the benzene π-system. The present experimental results are most readily explained using a recently proposed model of substituent effects in the benzene sandwich dimer in which the π-system of the substituted benzene is relatively unimportant and substituent effects arise from direct through-space interactions. Specifically, these results are the first experiments to clearly show that OMe enhances these π-stacking interactions, despite being a π-electron donor. This is in conflict with popular models in which substituent effects in aryl−aryl interactions are modulated by polarization of the aryl π-system.

Introduction

Noncovalent interactions (hydrogen bonding, π-stacking, cation-π, etc.) are of profound importance in molecular biology, drug design, and supramolecular chemistry.[1,2] Among noncovalent interactions, π-stacking interactions are perhaps the least well-characterized but are key to understanding myriad phenomena. Intramolecular through-space $\pi-\pi$ interactions have been used to alter electronic and optical properties of conjugated polymers,[3,4] and intermolecular π-stacking interactions were recently exploited by Chen and McNeil in the design of a novel analyte-triggered gelation.[5] Arene−arene interactions play a vital role in the structures and properties of DNA and RNA, in addition to the tertiary structures of proteins.[6] Interactions with aromatic amino acid side chains contribute to substrate binding in enzymes and were recently utilized[7] in the computational enzyme design of a Kemp elimination catalyst. Finally, complexation of aromatic amino acid side chains with DNA bases mediates DNA binding in anti-DNA autoantibodies, which are involved in the pathogenesis of the autoimmune disease systemic lupus erythematosus.[8]

There are four prototypical structures generally considered for the simplest $\pi-\pi$ stacked system, the benzene dimer (see Figure 1). Benchmark ab initio results[9−13] indicate that the global minimum parallel displaced and T-shaped configurations

[†] University of California, Los Angeles.
[‡] Massachusetts Institute of Technology.
[§] Current address: Department of Chemistry, University of Michigan, Ann Arbor, MI 48109-1055.

(1) Waters, M. L. *Curr. Opin. Chem. Bio.* **2002**, *6*, 736–741. Meyer, E. A.; Castellano, R. K.; Diederich, F. *Angew. Chem., Int. Ed.* **2003**, *42*, 1210–1250. Hobza, P. *Phys. Chem. Chem. Phys.* **2008**, *10*, 2581–2583.
(2) Hunter, C. A.; Lawson, K. R.; Perkins, J.; Urch, C. J. *J. Chem. Soc., Perkin Trans. 2* **2001**, 651–669. Hunter, C. A.; Sanders, J. K. M. *J. Am. Chem. Soc.* **1990**, *112*, 5525–5534.
(3) Morisaki, Y.; Chujo, Y. *Angew. Chem., Int. Ed.* **2006**, *45*, 6430–6437. Morisaki, Y.; Chujo, Y. *Macromolecules* **2002**, *35*, 587–589. Morisaki, Y.; Ishida, T.; Chujo, Y. *Macromolecules* **2002**, *35*, 7872–7877. Wang, W.; Xu, J.; Lai, Y.-H.; Wang, F. *Macromolecules* **2004**, *37*, 3546–3553.
(4) McNeil, A. J.; Müller, P.; Whitten, J. E.; Swager, T. M. *J. Am. Chem. Soc.* **2006**, *128*, 12426–12427.
(5) Chen, J.; McNeil, A. J. *J. Am. Chem. Soc.* **2008**, *130*, 16496–16497.
(6) Saenger, W. *Principles of Nucleic Acid Structure*; Springer: New York, 1984. Burley, S. K.; Petsko, G. A. *Science* **1985**, *229*, 23–28.
(7) Röthlisberger, D.; Khersonsky, O.; Wollacott, A. M.; Jiang, L.; Dechancie, J.; Betker, J.; Gallaher, J. L.; Althoff, E. A.; Zanghellini, A.; Dym, O.; Albeck, S.; Houk, K. N.; Tawfik, D. S.; Baker, D. *Nature* **2008**, *453*, 190–195.
(8) Tanner, J. J.; Komissarov, A. A.; Deutscher, S. L. *J. Mol. Biol.* **2001**, *314*, 807–822. Stollar, B. D. *Clin. Immunol. Allergy* **1981**, *1*, 243–260. Jang, Y. J.; Stollar, B. D. *Cell. Mol. Life Sci.* **2003**, *60*, 309–320. Blatt, N. B.; Glick, G. D. *Pharmacol. Ther.* **1999**, *83*, 125–139.
(9) Sinnokrot, M. O.; Sherrill, C. D. *J. Am. Chem. Soc.* **2004**, *126*, 7690–7697.
(10) Sinnokrot, M. O.; Valeev, E. F.; Sherrill, C. D. *J. Am. Chem. Soc.* **2002**, *124*, 10887–10893.
(11) Sinnokrot, M. O.; Sherrill, C. D. *J. Phys. Chem. A* **2006**, *110*, 10656–10668. Sherrill, C. D. In *Reviews in Computational Chemistry*; Lipkowitz, K. B., Cundari, T. R., Eds.;:Wiley-VCH: New York, 2009; Vol. 26, pp 1−38.
(12) Janowski, T.; Pulay, P. *Chem. Phys. Lett.* **2007**, *447*, 27–32.
(13) Dinadayalane, T. C.; Leszczynski, *J. Struct. Chem.* **2009**, *20*, 11–20.

 10.1021/ja903653j

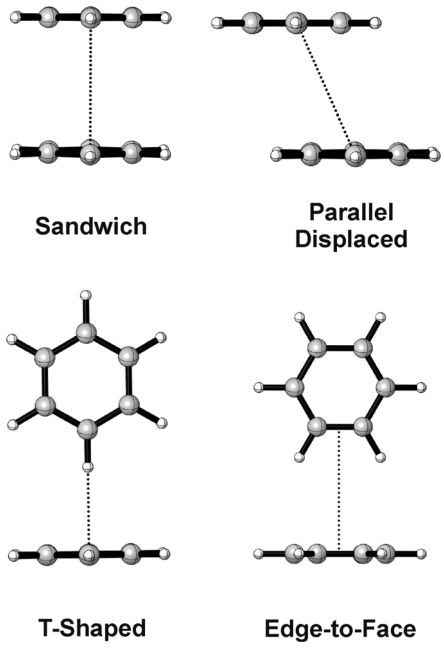

Figure 1. Prototypical benzene dimer configurations.

are essentially isoenergetic and bound by 2.7 kcal mol^{-1}. The sandwich configuration lies about 1 kcal mol^{-1} higher in energy. Although the sandwich form is not a stable minimum for the unsubstituted benzene dimer, this is a popular model system for theoretical studies of substituent effects.[9,11,14−22]

The prevailing view of substituent effects in the benzene dimer is the polar/π model[23] espoused by Cozzi and Siegel[24−27] and Hunter et al.[2] This intuitive electrostatic model enjoys broad acceptance in the literature, despite numerous theoretical studies critical of this simple picture.[9,11,16–22,28] In the polar/π model, electron-withdrawing substituents diminish the electron density in the π-cloud of the substituted ring, which decreases the electrostatic repulsion with the π-system of the interacting ring. The stacking interaction relative to the unsubstituted dimer is consequently enhanced. Conversely, π-electron-donating substituents result in weaker $\pi-\pi$ interactions. These general trends have been born out in many experiments, ranging from studies of intramolecular stacking interactions in conformationally flexible systems[24–27,29−31] to supramolecular host−guest complex experiments.[32−34] Gung and co-workers[30] utilized triptycene derivatives to study substituent effects in the parallel displaced dimer based on measured equilibria between conformations with stacked and unstacked aryl rings. Cozzi and Siegel[24–27] have introduced a number of experimental probes, including conformationally restricted polycyclic compounds yielding relative binding free energies of substituted parallel displaced dimers.[26] Hunter and co-workers[33,34] have quantified substituent effects on stacking interactions based on chemical double mutant cycle studies using supramolecular "zipper" complexes. Results from each of these experimental probes purportedly support the polar/π model. However, as discussed below, the data of Gung and co-workers[30] and Hunter et al.[33] are also consistent with an alternative model.[21] The work of Cozzi and Siegel,[24–27] on the other hand, clearly indicates that π-electron donors (CH_3, OCH_3, etc.)[35] decrease the π-stacking interaction in the benzene dimer, whereas electron-withdrawing substituents (CN, NO_2, etc.) enhance the interaction, in accord with the polar/π model.

Gas-phase ab initio computations paint a different picture.[17] The coupled cluster theory results of Sinnokrot and Sherrill[9,11,17] revealed enhanced stacking interactions in the sandwich dimer for all substituents studied, regardless of the electron-withdrawing or electron-donating character. Similar findings have also been reported by Kim et al.[16] and Ringer et al.[18] further demonstrated the additivity of substituent effects in multiply substituted benzene heterodimers. Additivity in the case of fluorine substitution has also been shown experimentally by Gung and co-workers.[36] Such strict additivity is contrary to expectations if π-polarization were the dominant cause of substituent effects, because the incremental polarization of the aryl π-system should decrease with each additional substituent.

(14) Gung, B. W.; Amicangelo, J. C. *J. Org. Chem.* **2006**, *71*, 9261–9270. Godfrey-Kittle, A.; Cafiero, M. *Int. J. Quantum Chem.* **2006**, *106*, 2035–2043. Smith, T.; Slipchenko, L. V.; Gordon, M. S. *J. Phys. Chem. A* **2008**, *112*, 5286–5294. Beg, S.; Waggoner, K.; Ahmad, Y.; Watt, M.; Lewis, M. *Chem. Phys. Lett.* **2008**, *455*, 98–102. Lee, E. C.; Hong, B. H.; Lee, J. Y.; Kim, J. C.; Kim, D.; Kim, Y.; Tarakeshwar, P.; Kim, K. S. *J. Am. Chem. Soc.* **2005**, *127*, 4530–4537.
(15) Grimme, S.; Antony, J.; Schwabe, T.; Mück-Lichtenfeld, C. *Org. Biomol. Chem.* **2007**, *5*, 741–758.
(16) Lee, E. C.; Kim, D.; Jurečka, P.; Tarakeshwar, P.; Hobza, P.; Kim, K. S. *J. Phys. Chem. A* **2007**, *111*, 3446–3457.
(17) Sinnokrot, M. O.; Sherrill, C. D. *J. Phys. Chem. A* **2003**, *107*, 8377–8379.
(18) Ringer, A. L.; Sinnokrot, M. O.; Lively, R. P.; Sherrill, C. D. *Chem.—Eur. J.* **2006**, *12*, 3821–3828.
(19) Arnstein, S. A.; Sherrill, C. D. *Phys. Chem. Chem. Phys.* **2008**, *10*, 2646–2655.
(20) Ringer, A. L.; Sherrill, C. D. *J. Am. Chem. Soc.* **2009**, *131*, 4574–4575.
(21) Wheeler, S. E.; Houk, K. N. *J. Am. Chem. Soc.* **2008**, *130*, 10854–10855.
(22) Wheeler, S. E.; Houk, K. N. *Mol. Phys.* **2009**, *107*, 749–760.
(23) This model is also often referred to as the Hunter−Sanders rules.
(24) Cozzi, F.; Cinquini, M.; Annunziata, R.; Dwyer, T.; Siegel, J. S. *J. Am. Chem. Soc.* **1992**, *114*, 5729–5733.
(25) Cozzi, F.; Siegel, J. S. *Pure Appl. Chem.* **1995**, *67*, 683–689.
(26) Cozzi, F.; Annunziata, R.; Benaglia, M.; Cinquini, M.; Raimondi, L.; Baldridge, K. K.; Siegel, J. S. *Org. Biomol. Chem.* **2003**, *1*, 157–162.
(27) Cozzi, F.; Annunziata, R.; Benaglia, M.; Baldridge, K. K.; Aguirre, G.; Estrada, J.; Sritana-Anant, Y.; Siegel, J. S. *Phys. Chem. Chem. Phys.* **2008**, *10*, 2686–2694.
(28) Müller-Dethlefs, K.; Hobza, P. *Chem. Rev.* **2000**, *100*, 143–168. Grimme, S. *Angew. Chem., Int. Ed.* **2008**, *47*, 3430–3434.
(29) Rashkin, M. J.; Waters, M. L. *J. Am. Chem. Soc.* **2002**, *124*, 1860–1861.
(30) Gung, B. W.; Xue, X.; Reich, H. J. *J. Org. Chem.* **2005**, *70*, 3641–3644.
(31) Gung, B. W.; Patel, M.; Xue, X. *J. Org. Chem.* **2005**, *70*, 10532–10537. Cubberley, M. S.; Iverson, B. L. *J. Am. Chem. Soc.* **2001**, *123*, 7560–7563. Newcomb, L. F.; Gellman, S. H. *J. Am. Chem. Soc.* **1994**, *116*, 4993–4994. Gardner, R. R.; McKay, S. L.; Gellman, S. H. *Org. Lett.* **2000**, *2*, 2335–2338. McKay, S. L.; Haptonstall, B.; Gellman, S. H. *J. Am. Chem. Soc.* **2001**, *123*, 1244–1245.
(32) Gray, M.; Goodman, A. J.; Carroll, J. B.; Bardon, K.; Markey, M.; Cooke, G.; Rotello, V. M. *Org. Lett.* **2004**, *6*, 385–388. Raraoni, R.; Blanzat, M.; Kubicek, S.; Braun, C.; Schweizer, W. B.; Gramlich, V.; Diederich, F. *Org. Biomol. Chem.* **2004**, *2*, 1962–1964. Yajima, T.; Takamido, R.; Shimazaki, Y.; Odani, A.; Nakabayashi, Y.; Yamauchi, O. *Dalton Trans.* **2007**, 299–307.
(33) Cockroft, S. L.; Hunter, C. A.; Lawson, K. R.; Perkins, J.; Urch, C. J. *J. Am. Chem. Soc.* **2005**, *127*, 8594–8595.
(34) Cockroft, S. L.; Perkins, J.; Zonta, C.; Adams, H.; Spey, S. E.; Low, C. M. R.; Vinter, J. G.; Lawson, K. R.; Urch, C. J.; Hunter, C. A. *Org. Biomol. Chem.* **2007**, *5*, 1062–1080. Cockroft, S. L.; Hunter, C. A. *Chem. Soc. Rev.* **2007**, *36*, 172–188.
(35) Although some authors dismiss OMe as a π-donor in this context on the basis of computed electrostatic potential plots, this is actually due to false assumptions regarding substituent effects on arene ESPs. See: Wheeler, S. E.; Houk, K. N. *J. Chem. Theory Comput.* **2009**, *5*, 2301–2312.
(36) Gung, B. W.; Xue, X.; Zou, Y. *J. Org. Chem.* **2007**, *72*, 2469–2475.

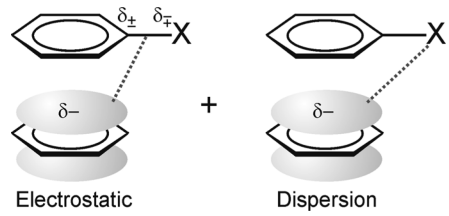

Figure 2. Direct-interaction model of substituent effects in the sandwich configuration of the benzene dimer.[21]

Wheeler and Houk examined substituent effects in the sandwich and edge-to-face configurations of the gas-phase benzene dimer.[21,22] For the sandwich dimer, the π-system of the substituted aryl ring is not necessary to recover substituent effects across a diverse set of substituents.[21,37] Instead, substituent effects were shown to arise from direct electrostatic and dispersion interactions between the substituent and the unsubstituted ring (see Figure 2). Rashkin and Waters[29] had previously invoked direct interactions between the substituent and the unsubstituted ring to account for experimental data on substituted parallel displaced benzene dimers. Sherrill and co-workers[18] attributed anomalous substituent effects in T-shaped benzene dimers to direct interactions.

A consequence of the "direct-interaction" model[21] is that σ-withdrawing character dominates substituent effects in the benzene dimer, not the extent to which substituents donate or accept π-electrons. Specifically, whereas the polar/π model[2,24,27] predicts that π-donors[35] such as OMe should hinder the stacking interaction relative to the unsubstituted dimer, this new model[21] maintains that OMe enhances the interaction as a result of its net withdrawing inductive/field character (the field and resonance parameters for OMe are $F = 0.29$ and $R = -0.56$, respectively).[38,39] Similarly, while the polar/π model predicts a correlation of stacking interactions with σ_p, the direct-interaction model is based on a correlation with σ_m.

A major lingering discrepancy between experimental results and gas-phase computations is the role of dispersion interactions. Sherrill and co-workers[20] have stressed the importance of dispersion in substituent effects in the sandwich dimer, although there is no evidence of a significant role for dispersion in available experiments.[33,40] Cockroft and Hunter[40] recently tackled this issue in an elegant paper on the role of solvent effects in edge-to-face aromatic interactions. Ultimately, it was concluded that "electrostatic effects play a dominant role in determining the properties of aromatic interactions in organic solvents," and the predicted importance of dispersion in gas-phase computations arises from the neglect of solvent effects.

Here we present stereoselective Diels–Alder reactions (Scheme 1) that probe substituent effects in the sandwich configuration of the benzene dimer. These reactions are based on a similar stereoselective transformation utilized by Swager and co-workers in the synthesis of conjugated polymers incorporating π-stacking interactions along the polymer backbone.[4] In contrast to previous experimental probes, the current approach quantifies substituent effects through barrier height differences of competing transition states to provide relative stacking free energies for substituted and unsubstituted benzene dimers. Computational examination of the transition states and related model systems demonstrate that the product distributions reflect differential aryl–aryl interactions.

Experimental Methods

Substrates **1a**–**1d** were prepared in two steps from substituted anthracenes and dimethyl acetylenedicarboxylate (see Supporting Information). The Diels–Alder reactions were performed in decane because of its high boiling point and nonpolar nature. Importantly, both starting materials were soluble at the reaction temperature (150 °C). Excess anthracene (10 equiv) was found to provide higher yields. The major products (**2a**, **3b**, **2c**, and **2d**) were characterized by single-crystal X-ray analysis (see Supporting Information). The product ratios were then determined by integrating the bridgehead protons in the crude reaction mixtures via ^{1}H NMR spectroscopy. Average isolated yields ranged from 62% for substrate **1b** to 77% for **1d**. Observed product ratios varied from 1:2 to 1:4 for **1b**, 4:1 to 6:1 for **1c**, and 12:1 to 20:1 for **1d**. The average of the measured product ratios is reported.

To verify that the product ratios reflect the kinetic selectivity (i.e., free energy differences in the transition states) and not the thermodynamic stability of the two products, we subjected product **2a** to the reaction conditions using an excess of 1,4-dibromoanthracene. No crossover products were detectable by ^{1}H NMR after 24 h, indicating no retro-Diels–Alder reaction was occurring. Similarly, product **2c** was combined with excess anthracene and heated to 150 °C. NMR revealed no formation of product **3c** after 24 h. These findings are consistent with computed free energy barriers for the reverse reactions, which are all in excess of 40 kcal mol^{-1} at the M05-2X/6-31+G(d) level of theory. The reported product ratios are not the result of an equilibration.

Theoretical Methods

Structures of the reactants, products, and associated transition states for the Diels–Alder reactions in Scheme 1 were optimized using the B3LYP and M05-2X density functional theory (DFT) functionals[41,42] paired with either the 6-31+G(d) or AVDZ′ basis sets. Two additional substrates [**1e** (Cl) and **1f** (F)] were also examined computationally. For each substrate (**1a**–**1f**), transition states leading to products **2** and **3** were located, denoted by **TS2** and **TS3**, respectively. M06-2X/6-31+G(d) single point energies[43] were computed at M05-2X geometries. There is no published 6-31+G(d) basis set for Br. When the M05-2X and M06-2X functionals are paired with the built-in 6-31+G(d) Br basis set in Gaussian03,[44] interaction energies for the $C_6H_5Br\cdots C_6H_6$ sandwich dimer are overestimated by 2–3 kcal mol^{-1}. Consequently, the AVDZ′ basis set[9] was used for all systems that include Br. This basis set comprises the cc-pVDZ basis set on hydrogen and the aug-cc-pVDZ basis set without diffuse *d*-functions for other atoms.[45]

Harmonic vibrational frequencies were computed for all optimized structures to characterize the stationary points. Even though B3LYP predicts C_s-symmetric transition states, M05-2X yields nonsymmetric structures for **TS3** for all substituents as well as **TS2a** and **TS2b**. In these cases, the C_s-symmetric structures have an additional small (<20 cm^{-1}) imaginary vibrational frequency corresponding to rotation of the anthracene relative to the substrate. The energy differences between the C_s- and C_1-symmetric stationary

(37) Wheeler, S. E.; Houk, K. N. *J. Chem. Theory Comput.* **2009**, *5*, 2301–2312.
(38) Roberts, J. D.; Moreland, W. T. *J. Am. Chem. Soc.* **1953**, *75*, 2167–2173. Taft, R. W. *J. Phys. Chem.* **1960**, *64*, 1805–1815. Swain, C. G.; Lupton, E. C. *J. Am. Chem. Soc.* **1968**, *90*, 4328–4337.
(39) Hansch, C.; Leo, A.; Taft, R. W. *Chem. Rev.* **1991**, *91*, 165–195.
(40) Cockroft, S. L.; Hunter, C. A. *Chem. Commun.* **2009**, 3961–3963.
(41) Becke, A. D. *J. Chem. Phys.* **1993**, *98*, 5648–5652.
(42) Zhao, Y.; Schultz, N. E.; Truhlar, D. G. *J. Chem. Theory Comput.* **2006**, *2*, 364–382.
(43) Zhao, Y.; Truhlar, D. G. *Theor. Chem. Acc.* **2008**, *120*, 215–241.
(44) Frisch, M. J. et al. *Gaussian 03, Revision E.01*; Gaussian, Inc.: Wallingford, CT, 2004.
(45) Dunning, T. H., Jr. *J. Chem. Phys.* **1989**, *90*, 1007–1023. Kendall, R. A.; Dunning, T. H., Jr.; Harrison, R. J. *J. Chem. Phys.* **1992**, *96*, 6796–6806.

Scheme 1

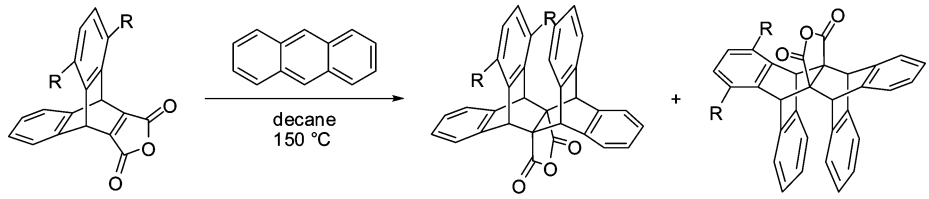

1a: R = H
1b: R = Me
1c: R = OMe
1d: R = Br

2a: R = H
2b: R = Me
2c: R = OMe
2d: R = Br

3b: R = Me
3c: R = OMe
3d: R = Br

Table 1. Interaction Energies (kcal mol^{-1}) for $C_6H_6\cdots C_6H_5R$ Benzene Sandwich Dimers, Relative to the Unsubstituted Benzene Dimer[a]

	Me	OH	OMe	F	Cl	Br	CN
M05-2X	0.3	0.4	0.3	0.5	0.8	1.0[b]	1.3
M06-2X	0.4	0.5	0.6	0.6	1.0	1.1[b]	1.4
CCSD(T)[c]	0.5[d]	0.4[d]	0.6[e]	0.5[d]	0.9[e]	1.1[e]	1.3[d]

[a] Positive numbers indicate enhanced interaction relative to the unsubstituted dimer. The interaction energy for the unsubstituted benzene dimer is −0.5 and −1.0 kcal mol^{-1} at the M05-2X/6-31+G(d) and M06-2X/6-31+G(d) levels of theory, respectively. The M05-2X/AVDZ′ and M06-2X/AVDZ′ values are −0.7 and −1.6, respectively. The CCSD(T) value from ref 9 is −1.8 kcal mol^{-1}. [b] AVDZ′ basis set. [c] Estimated CCSD(T)/aug-cc-pVTZ. [d] From ref 9. [e] This work.

points were all small (<0.1 kcal mol^{-1}). Free energy corrections (423 K) were computed within the rigid-rotor/harmonic-oscillator approximation using unscaled harmonic vibrational frequencies at the corresponding level of theory. Effects of solvent were approximately accounted for using the conductor-like polarizable continuum model (CPCM)[46] with solvent parameters for heptane ($\varepsilon = 1.92$, $R_{solv} = 3.125$ Å). M05-2X/6-31+G(d) free energy corrections and solvent corrections were appended to the M06-2X electronic energies.

Fine DFT integration grids (70 radial and 590 angular points) were utilized in all M05-2X and M06-2X computations, because it has previously been demonstrated that these functionals are particularly sensitive to integration grid density, particularly when applied to weakly bound complexes.[47] B3LYP and M05-2X optimizations and frequencies were carried out using Guasisan03.[44] M06-2X single point energies and constrained M05-2X optimizations on truncated structures were computed using NWChem 5.1.[48,49]

Results and Discussion

The Diels−Alder reactions in Scheme 1 have been examined experimentally and using modern DFT methods[42,43,50] to probe substituent effects in face-to-face aryl−aryl interactions. These reactions pose a number of difficulties for the application of standard theoretical methods. The size of the systems in Scheme 1 (63 atoms in **2c**, for example) precludes the application of rigorous ab initio approaches. On the other hand, the application of DFT is hampered by the need to account for the dispersion effects governing the π-stacking interactions present in **TS2** and **TS3**. Popular DFT functionals (and B3LYP in particular) predict repulsive interaction potentials for the sandwich configuration of the benzene dimer.[51] However, progress has been made in the parametrization of new functionals[42,43,50] and the development of empirical corrections to existing functionals,[15,52] opening up numerous areas of applications that were previously untenable for DFT. For example, Grimme and co-workers[15] recently demonstrated the utility of empirical dispersion corrections to standard DFT functionals in capturing substituent effects in the triptycene-based probe of Gung and co-workers.[30]

Validation of the Theoretical Approach. Previous benchmark studies[42,43,50,53] have demonstrated that the M05-2X and M06-2X DFT functionals[42,43] provide a satisfactory description of prototypical π-stacking interactions. These functionals were applied to $C_6H_6\cdots C_6H_5R$ sandwich dimers and compared to benchmark coupled cluster results to assess their performance for substituted benzene dimers. These benchmark values, which are estimates of CCSD(T)/aug-cc-pVTZ interaction energies, arise from counterpoise-corrected CCSD(T)/AVDZ′ energies corrected for basis set incompleteness at the MP2 level of theory.[54] All interaction energies were computed within the frozen monomer approximation. Monomer geometries were

(46) Barone, V.; Cossi, M. *J. Phys. Chem. A* **1998**, *102*, 1995–2001.
(47) Gräfenstein, J.; Cremer, D. *J. Chem. Phys.* **2007**, *127*, 164113. Gräfenstein, J.; Izotov, D.; Cremer, D. *J. Chem. Phys.* **2007**, *127*, 214103. Johnson, E. R.; Becke, A.; Sherrill, C. D.; DiLabio, G. A. *J. Chem. Phys.* **2009**, *131*, 034111. Wheeler, S. E.; Houk, K. N. *J. Chem. Theory Comput.* **2010**, *6*, 395–404.
(48) Bylaska, E. J.; et al. *NWChem, A Computational Chemistry Package for Parallel Computers, Version 5.1*; Pacific Northwest National Laboratory: Richland, WA, 2007.
(49) Kendall, R. A.; Apra, E.; Bernholdt, D. E.; Bylaska, E. J.; Dupuis, M.; Fann, G. I.; Harrison, R. J.; Ju, J.; Nichols, J. A.; Nieplocha, J.; Straatsma, T. P.; Windus, T. L.; Wong, A. T. *Comput. Phys. Commun.* **2000**, *128*, 260–283.
(50) Zhao, Y.; Truhlar, D. G. *J. Chem. Theory Comput.* **2007**, *3*, 289–300. Zhao, Y.; Truhlar, D. G. *Acc. Chem. Res.* **2008**, *41*, 157–167.
(51) Johnson, E. R.; Wolkow, R. A.; DiLabio, G. A. *Chem. Phys. Lett.* **2004**, *394*, 334–338.
(52) Schwabe, T.; Grimme, S. *Phys. Chem. Chem. Phys.* **2007**, *9*, 3397–3406. Tapavicza, E.; Lin, I.-C.; von Lilienfeld, A.; Tavernelli, I.; Coutinho-Neto, M. D.; Rothlisberger, U. *J. Chem. Theory Comput.* **2007**, *3*, 1673–1679. Grimme, S. *J. Comput. Chem.* **2004**, *25*, 1463–1473. Grimme, S. *J. Comput. Chem.* **2006**, *27*, 1787–1799. Kubař, T.; Jurečka, P.; Černey, J.; Řezáč, J.; Otyepka, M.; Valdés, H.; Hobza, P. *J. Phys. Chem. A* **2007**, *111*, 5642–5647. Jurečka, P.; Šponer, J.; Černey, J.; Hobza, P. *Phys. Chem. Chem. Phys.* **2006**, *8*, 1985–1993. Jurečka, P.; Černey, J.; Hobza, P.; Salahub, D. R. *J. Comput. Chem.* **2007**, *28*, 555–569. Wu, Q.; Yang, W. *J. Chem. Phys.* **2002**, *116*, 515–524. Zhechkov, L.; Heine, T.; Patchkovskii, S.; Seifert, G.; Duarte, H. A. *J. Chem. Theory Comput.* **2005**, *1*, 841–847. Zimmerli, U.; Parrinello, M.; Koumoutsakos, P. *J. Chem. Phys.* **2004**, *120*, 2693–2699.
(53) Zhao, Y.; Truhlar, D. G. *Phys. Chem. Chem. Phys.* **2005**, *7*, 2701–2705. Hohenstein, E. G.; Chill, S. T.; Sherrill, C. D. *J. Chem. Theory Comput.* **2008**, *4*, 1996–2000.
(54) Estimated CCSD(T)/aug-cc-pVTZ = CCSD(T)/AVDZ′ + (MP2/aug-cc-pVTZ - MP2/AVDZ′).

Table 2. Predicted Solvent-Corrected (CPCM) Free Energy Barriers ($\Delta G^{\ddagger}$, 423 K), Free Energy Barrier Differences [$\Delta\Delta G^{\ddagger} = \Delta G^{\ddagger}$(**TS3**) − $\Delta G^{\ddagger}$(**TS2**)], and Experimentally Measured **2**:**3** Ratios and Corresponding $\Delta\Delta G^{\ddagger}$ Values[a]

		M05-2X		M06-2X		B3LYP		experiment	
product		$\Delta G^{\ddagger}$	$\Delta\Delta G^{\ddagger}$	$\Delta G^{\ddagger}$	$\Delta\Delta G^{\ddagger}$	$\Delta G^{\ddagger}$	$\Delta\Delta G^{\ddagger}$	**2**:**3** ratio	$\Delta\Delta G^{\ddagger}$
H	**2a**	38.1		37.4		58.5			
Me	**2b**	36.7		35.4		60.5			
	3b	36.7	0.0	36.1	0.3	59.8	−0.7	1:3	−0.9
OMe	**2c**	37.1		36.2		61.0			
	3c	38.9	1.8	38.2	2.0	60.8	−0.2	5:1	1.4
Br	**2d**	33.1		32.6		60.8			
	3d	34.4	1.3	34.2	1.7	60.6	−0.2	17:1	2.4
Cl	**2e**	28.4		27.5		58.9			
	3e	30.6	2.2	29.9	2.4	59.8	0.9	[b]	[b]
F	**2f**	35.4		34.9		58.3			
	3f	38.4	2.9	37.8	2.9	59.0	0.7	[b]	[b]

[a] All energies given in kcal mol^{-1}. AVDZ′ basis set used for substrates **2d** and **3d**. 6-31+G(d) basis set used for the remaining systems. [b] Substrates **1e** and **1f** were not tested experimentally.

optimized at the MP2/aug-cc-pVTZ level of theory for the CCSD(T) computations. Table 1 shows that M05-2X and M06-2X, when paired with a double-ζ quality basis sets, provide very accurate relative interaction energies for substituted benzene sandwich dimers.

Accurate activation barriers are also desirable in the theoretical treatment of the reactions in Scheme 1. Computed free energy barriers and reaction free energies for the 1,4-cycloaddition of maleic anhydride and benzene are given in Table S6 in Supporting Information, computed using M05-2X, M06-2X, and B3LYP paired with the 6-31+G(d) basis set. These DFT results are compared to benchmark CBS-QB3 predictions.[55] The M05-2X and M06-2X functionals offer a reliable description of this reaction, with the M05-2X-predicted barrier (35.5 kcal mol^{-1}) falling within 0.7 kcal mol^{-1} of the CBS-QB3 value of 34.8 kcal mol^{-1}. The B3LYP functional overestimates the free energy barrier by almost 15 kcal mol^{-1}. B3LYP similarly predicts the reaction free energy to be too large by 18 kcal mol^{-1}, whereas the M05-2X and M06-2X predictions of 11.0 and 12.4 kcal mol^{-1} are in good agreement with the CBS-QB3 value (11.6 kcal mol^{-1}). These failures of B3LYP and apparent success of M05-2X and M06-2X for this cycloaddition are in accord with recent findings of Pieniazek and co-workers.[56]

Because both substituent effects on aryl−aryl interactions and activation barriers are shown to be treated properly with M05-2X, this functional is used primarily for the reactions depicted in Scheme 1.

Product Distributions. Experimental product ratios for the reactions in Scheme 1 are provided in Table 2, along with the corresponding relative free energy barriers ($\Delta\Delta G^{\ddagger}$) derived from classical transition state theory. All substituents lead to pronounced stereoselectivity. Solvent-corrected free energy barriers and relative barriers from M05-2X, M06-2X, and B3LYP are also provided in Table 2. Overall, the M05-2X- and M06-2X-predicted $\Delta\Delta G^{\ddagger}$ values are in only modest agreement with the experimental results. In the case of **1b**, M05-2X predicts no selectivity, but experimentally product **3b** is favored over **2b** 3:1. For **1d**, M05-2X and M06-2X underestimate the experimentally derived $\Delta\Delta G^{\ddagger}$ value of 2.4 kcal mol^{-1}. The B3LYP free energies are in poorer agreement with the experimental data, predicting the opposite stereoselectivity for the OMe- and Br-substituted substrates than observed experimentally, although for **1d** the B3LYP $\Delta\Delta G^{\ddagger}$ value of −0.7 kcal mol^{-1} is fortuitously in very good agreement with the experimental value (−0.9 kcal mol^{-1}). In accord with the findings for the parent cycloaddition, B3LYP drastically overestimates these reaction barriers, predicting activation energies exceeding 60 kcal mol^{-1} in some cases. Despite the nonpolar nature of the solvent, CPCM corrections to the free energy barriers are significant. Solvent corrections generally increase both barriers, but **TS2** is affected to a greater extent. The net impact on the $\Delta\Delta G^{\ddagger}$ values ranges from −0.1 to −2.8 kcal mol^{-1}.

Table 3. Predicted Gas-Phase Enthalpy Barriers ($\Delta H^{\ddagger}$, 423 K) and Enthalpy Barrier Differences [$\Delta\Delta H^{\ddagger} = \Delta H^{\ddagger}$(**TS3**) − $\Delta H^{\ddagger}$(**TS2**)][a]

		M05-2X		M06-2X		B3LYP	
product		$\Delta H^{\ddagger}$	$\Delta\Delta H^{\ddagger}$	$\Delta H^{\ddagger}$	$\Delta\Delta H^{\ddagger}$	$\Delta H^{\ddagger}$	$\Delta\Delta H^{\ddagger}$
H	**2a**	13.2		12.5		35.4	
Me	**2b**	12.3		11.4		35.8	
	3b	12.4	0.1	11.7	0.4	35.1	−0.7
OMe	**2c**	11.3		10.5		34.6	
	3c	13.9	2.5	13.2	2.7	36.0	1.3
Br	**2d**	9.0		8.6		32.8	
	3d	12.5	3.4	12.3	3.8	34.9	2.1
Cl	**2e**	9.3		8.4		33.0	
	3e	12.5	3.2	11.8	3.4	35.2	2.2
F	**2f**	10.3		9.7		33.0	
	3f	12.8	2.5	12.2	2.5	35.1	2.1

[a] All energies given in kcal mol^{-1}. AVDZ′ basis set used for substrates **2d** and **3d**. 6-31+G(d) basis set used for the remaining systems.

Computed gas-phase relative enthalpy barriers ($\Delta\Delta H^{\ddagger}$, Table 3) exhibit much better agreement with experiment, indicating possible problems with the free energy predictions in Table 2. For systems of this size, free energy corrections computed using the standard rigid-rotor/harmonic-oscillator approximation can be problematic, particularly given the presence of very small vibrational frequencies. These small frequencies are not satisfactorily treated as harmonic oscillators and small changes in these frequencies lead to large shifts in predicted entropy contributions, exaggerating otherwise inconsequential errors in computed frequencies.

The M05-2X and M06-2X $\Delta\Delta H^{\ddagger}$ values are consistently 1.0 ± 0.1 and 1.3 ± 0.1 kcal mol^{-1} larger than the experimental $\Delta\Delta G^{\ddagger}$ values. The B3LYP-predicted gas-phase relative enthalpy barriers are in very good agreement with the experimental data, deviating by no more than 0.3 kcal mol^{-1}. A primary difference between the M05-2X and M06-2X methods and the B3LYP functional is the recovery of dispersion-like interactions by the former methods. The differences between the M05-2X- and B3LYP-predicted $\Delta\Delta H^{\ddagger}$ values in Table 3 are consistent with the expected size of the dispersion contribution to these relative barriers from the substituents.[9] This is demonstrated most clearly by the series of halogen-substituted substrates (**1d**−**1f**). The M05-2X-predicted enthalpy differences decrease across the series Br > Cl > F and follow the trend in polarizabilities. The B3LYP functional predicts essentially the same $\Delta\Delta H^{\ddagger}$ values for all three of these species, failing to account for expected differences in dispersion interactions.

The systematic deviation of the M05-2X and M06-2X results from the experimental $\Delta\Delta G^{\ddagger}$ values suggests that dispersion

(55) Montgomery, J. A., Jr.; Frisch, M. J.; Ochterski, J. W.; Petersson, G. A. *J. Chem. Phys.* **2000**, *112*, 6532–6542. Montgomery, J. A., Jr.; Frisch, M. J.; Ochterski, J. W.; Petersson, G. A. *J. Chem. Phys.* **1999**, *110*, 2822–2827. Guner, V.; Khuong, K. S.; Leach, A. G.; Lee, P. S.; Bartberger, M. D.; Houk, K. N. *J. Phys. Chem. A* **2003**, *107*, 11445–11459. Ess, D. H.; Houk, K. N. *J. Phys. Chem. A* **2005**, *109*, 9542–9553.

(56) Pieniazek, S. N.; Clemente, F.; Houk, K. N. *Angew. Chem., Int. Ed.* **2008**, *47*, 7746–7749.

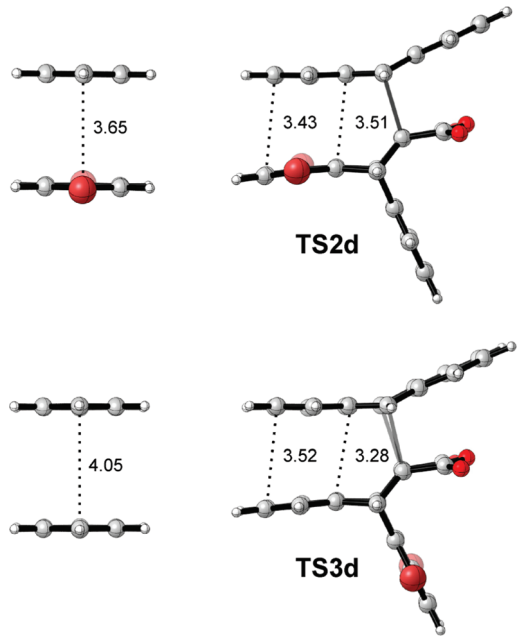

Figure 3. Structures of **TS2d** and **TS3d** and corresponding gas-phase sandwich configurations of the dibromobenzene−benzene and benzene−benzene dimers, optimized at the M05-2X/6-31+G(d) level of theory.

interactions do not play a major role in the present experiment, in agreement with the recent reports of Cockroft and Hunter.[40] That the M06-2X results consistently deviate more from the experimental $\Delta\Delta G^{\ddagger}$ values than do the M05-2X enthalpies is also consistent with a lack of significant dispersion-like effects in the experiments, since M06-2X is known to provide a more complete recovery of dispersion effects compared with M05-2X.[57] Apparently, the very good agreement between the B3LYP $\Delta\Delta H^{\ddagger}$ values and the experimental data arises from the failure of that functional to account for the dispersion effects that are present in the gas-phase but attenuated in solution. In addition to the indirect effects of solvent on dispersion discussed by Cockroft and Hunter,[40] there is the potential for more direct solvent effects. It has previously been shown that the primary dispersion contribution to substituent effects in the gas-phase benzene sandwich dimer are the direct interactions between the substituent and the complexed ring.[21] The presence of a polarizable solvent between the substituents and the other ring could potentially distinguish these direct dispersion interactions.[58]

Origins of Barrier Height Differences. The contribution of π-stacking interactions to the energy difference between **TS2** and **TS3** ($\Delta\Delta E^{\ddagger}$) can be approximated by examining a series of model systems. In this way, it can be demonstrated that the product distributions for the reactions in Scheme 1 provide a reliable gauge of substituent effects in the benzene dimer. Figure 3 shows the M05-2X/6-31+G(d) structures for **TS2d** and **TS3d**, along with the gas-phase $C_6H_4Br_2\cdots C_6H_6$ and $C_6H_6\cdots C_6H_6$ sandwich dimers. The arrangements of the interacting aromatic rings in these transition states are congruent with the structures of the corresponding gas-phase dimers. Inter-ring distances for all of the optimized transition states are provided in Table S8 in Supporting Information along with the corresponding gas-phase dimer distances. The separations in the optimized transition states (averaging 3.4 Å) are somewhat smaller than benchmark gas-phase dimer distances (3.8 Å for the benzene dimer and slightly shorter for substituted dimers),[9–12,17,18] although they are comparable to the aryl−aryl distance in the parallel displaced benzene dimer.[10,11,19]

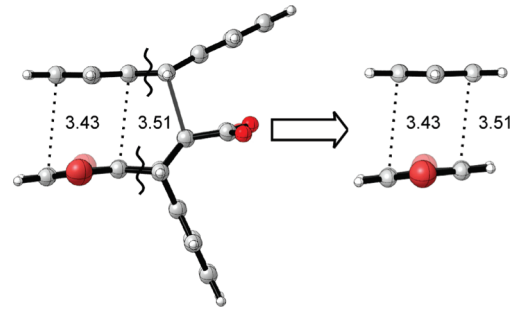

Figure 4. To isolate the relative π-stacking interactions in the transition states ($\Delta\Delta E_{\pi}$), the C−C bonds in the M05-2X optimized **TS2** and **TS3** structures were cut as indicated by the wavy lines and replaced with hydrogens to yield a benzene dimer with the same geometry as that present in each transition state.

Table 4. M05-2X Interaction Energies (kcal mol^{-1}) of 1,4-Disubstituted Benzene−Benzene Dimers Relative to the Unsubstituted Sandwich Dimer, Computed at the Geometries Present in **TS2** and **TS3** ($\Delta\Delta E_{\pi}$) and at the Optimized Gas-Phase Geometries ($\Delta\Delta E_{gas}$)[a]

substituent	ΔE_{stack}(TS1)	ΔE_{stack}(TS2)	$\Delta\Delta E_{\pi}$	$\Delta\Delta E_{gas}$
Me	1.2	1.7	0.4	0.6
OMe	0.5	1.8	1.3	0.8
Br	−1.6	1.3	2.9	2.3
Cl	−0.7	1.8	2.5	1.8
F	0.3	1.9	1.6	1.1

[a] The AVDZ′ basis set was used for dibromobenzene···benzene dimer. The 6-31+G(d) basis set was used otherwise.

The energetic cost of these differences in the stacking interactions in **TS2** and **TS3** compared to the corresponding gas-phase dimers can be quantified by removing the remainder of the TS atoms and replacing the open carbon valences with hydrogens, as depicted in Figure 4. The placement of the added hydrogens was optimized using M05-2X/6-31+G(d) while holding the remainder of the atoms fixed. Interaction energies at the geometries present in **TS2** and **TS3** [ΔE_{stack}(TS2) and ΔE_{stack}(TS3)] are included in Table 4. Except for the dibromobenzene and dichlorobenzene interactions present in **TS2d** and**TS2e**, the stacking interactions in the transition states are slightly repulsive energetically. This is attributed to the smaller interring distances in the transition states compared to the fully relaxed dimers. Relative interaction energies ($\Delta\Delta E_{stack}$) for the complexes present in **TS2** and **TS3** are also given in Table 4, along with interaction energies for $C_6H_4R_2\cdots C_6H_6$ dimers relative to the unsubstituted sandwich dimer ($\Delta\Delta E_{gas}$). The relative π-stacking interactions in **TS2** and **TS3** are in general agreement with the gas-phase dimer results and follow the same trend: Me < OMe < *F* < Cl < Br. The deviations in inter-ring distances in **TS2** and **TS3** compared to the corresponding gas-phase dimers have no substantial net effect on the relative stacking energies.

Minor complications can arise from secondary effects of the substituents on the underlying Diels−Alder reactions. The effects of the substituents on the computed transition state geometries are minor. For **TS2**, the length of the forming C−C bonds is 2.39 Å for all of the substituted substrates, compared

(57) Karton, A.; Tarnopolsky, A.; Lamre, J.-F.; Schatz, G. C.; Martin, J. M. L. *J. Phys. Chem. A* **2008**, *112*, 12868–12886.
(58) Donchev, A. G. *J. Chem. Phys.* **2006**, *125*, 074713.

Table 5. Approximate Decomposition of Computed Electronic Energy Barrier Differences ($\Delta\Delta E^{\ddagger}$) into π-Stacking ($\Delta\Delta E_{stack}$, see Figure 4) and Substituent Effects on the Underlying Diels−Alder Barriers ($\Delta\Delta E_{sub}$) for the Reactions in Scheme 1

substrate		$\Delta\Delta E^{\ddagger}$	≈	$\Delta\Delta E_{stack}$	+	$\Delta\Delta E_{sub}$
Me	**1b**	0.0		0.4		0.1
OMe	**1c**	2.6		1.3		1.0
Br	**1d**	3.5		2.9		0.9
Cl	**1e**	3.3		2.5		0.8
F	**1f**	2.6		1.6		0.3

to 2.41 Å for **TS2a**. For **TS3**, there is a larger variation in the length of the forming C−C bonds, ranging from 2.39 Å for the Me- and Br-substituted substrates to 2.44 Å for **TS3f**. However, the positions of the Diels−Alder transition states do not correlate with the observed selectivities and are not the origin of the barrier height differences. To quantify the effects of the substituents on the underlying Diels−Alder reaction barriers heights, the addition of 1,3-butadiene to substrates **1a**−**1f** was examined at the M05-2X/6-31+G(d) level of theory (see Scheme S1 and Table S9 in Supporting Information). The differences in electronic energy barriers ($\Delta\Delta E_{sub}$) for the two possible cycloadditions are given in Table 5. These substituent effects on the underlying Diels−Alder reaction will also be present in the reactions given in Scheme 1.

In **TS3** there is the potential for steric interactions between the substituents and the carbonyl oxygens of the maleic anhydride. In the computed transition state geometries the distance of the closest approaching atoms is always in excess of the corresponding van der Waals radii, and steric interactions are not contributing to the barrier height differences.

The contribution of π-stacking interactions ($\Delta\Delta E_{stack}$) and secondary substituent effects ($\Delta\Delta E_{sub}$) to the barrier height differences are given in Table 5, along with the differences in electronic energy barriers ($\Delta\Delta E^{\ddagger}$). For all of the substrates except **1f**, the sum of $\Delta\Delta E_{stack}$ and $\Delta\Delta E_{sub}$ is within 0.5 kcal mol^{-1} of $\Delta\Delta E^{\ddagger}$. For **1f** this difference is 0.7 kcal mol^{-1}. Apparently there are small additional effects that affect $\Delta\Delta E^{\ddagger}$ not accounted for by these simple models. Regardless, in each case the largest contributor to $\Delta\Delta E^{\ddagger}$ arises from differential π-stacking interactions and the measured product distributions provide a probe of substituent effects on π-stacking interactions.

Substituent Effects in the Benzene Dimer. The sandwich configuration of the benzene dimer is not a stable minimum, and both the parallel displaced and T-shaped structures are favored energetically. However, the sandwich dimer is the configuration most often studied theoretically[9,11,14–22] and is the configuration depicted in qualitative models of substituent effects espoused by both Cozzi and Siegel[24–27] and Hunter et al.[2] The present experimental probe provides a means of testing our understanding of substituent effects in aryl−aryl sandwich complexes. The rigidity of the transition structures leading to products **2** and **3** forces one ring of the incoming anthracene into a nearly parallel arrangement with an aromatic ring of the substrate at a distance comparable to that in the gas-phase sandwich dimers (see Figure 3). Although contaminating factors arise from secondary substituent effects and other perturbations, the bulk of the observed energy barrier differences is due to differential π-stacking interactions. Moreover, it was shown above (see Table 4) that the deviations in the stacking interactions in **TS2** and **TS3** from the ideal gas-phase benzene dimers have little net effect on the *relative* stacking energies. As a result, the measured free energy barrier differences ($\Delta\Delta G^{\ddagger}$) provide a measure of the relative interaction free energies ($\Delta\Delta G^{stack}$) of the substituted sandwich dimers.

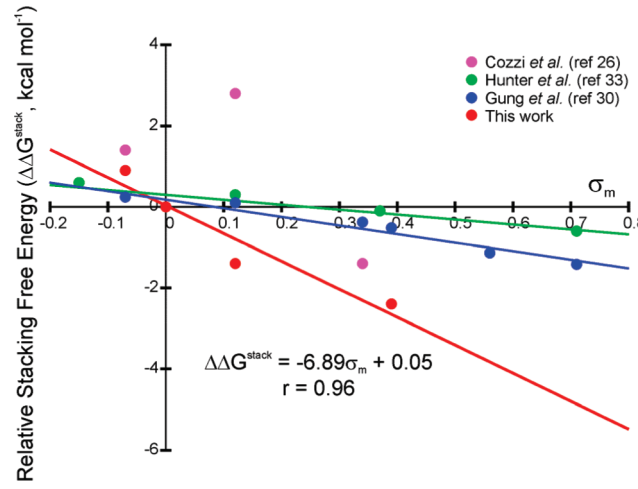

Figure 5. Experimental stacking free energies ($\Delta\Delta G^{stack}$, relative to R = H, in kcal mol^{-1}) versus σ_m for 1,4-disubstituted arene sandwich complexes.[39] The monosubstituted results of Cozzi and Siegel,[26] Hunter et al.,[33] and Gung et al.[30] were doubled to enable direct comparison with this work.

Experimental relative interaction free energies ($\Delta\Delta G^{stack}$) for the disubstituted dimers are plotted in Figure 5 as a function of the Hammett σ meta constants (σ_m). These constants primarily indicate the inductive electron-donating or -withdrawing character of the substituents.[39] There is a strong correlation (r = 0.96) between $\Delta\Delta G^{stack}$ and σ_m, in accord with recent theoretical results.[21] The primary difference between computed gas-phase interaction energies for the benzene sandwich dimer and these $\Delta\Delta G^{stack}$ values is that in the computations substituted dimers are stabilized by on average about 0.5 kcal mol^{-1} compared to the unsubstituted dimer. This is due to direct dispersion interactions[20,21] and leads to a y-intercept of −0.5 kcal mol^{-1} when plotting computed interaction energies versus σ_m.[21] In Figure 5, the y-intercept of the best fit line for the experimental stacking free energies is essentially zero. A consequence is that even though gas-phase computations predict that all substituents stabilize the benzene dimer, experimental results indicate a net repulsive interaction between paraxylene and benzene. The direct dispersion interactions arising in gas-phase computations are diminished in the experiments, presumably as a result of solvent effects.[40,58]

Experimental stacking free energies from Gung and co-workers,[30] Cozzi and Siegel,[27] and Hunter et al.[33] are also included in Figure 5. These experimental results have previously been shown to correlate well with σ_p (r = 0.98, 0.98, and 0.99 for Gung,[30] Cozzi,[27] and Hunter,[33] respectively), a feature used to support the polar/π model.[2,24–27] However, as seen in Figure 5, there is also a strong correlation between the data of Gung et al.[30] and Hunter and co-workers[33] with σ_m (r = 0.97 and 0.93, respectively). This correlation with both σ_m and σ_p arises from the similarity of σ_m and σ_p constants for most of the substituents studied in those works. The only substituent considered for which σ_m and σ_p differ qualitatively (OMe) exhibited such a small effect on the stacking interaction energy in these experiments that the sign of the effect on stacking interactions is unclear. The present experimental results show a clear correlation with σ_m, and the strong enhancement of the stacking interaction by OMe stymies any correlation with σ_p. On the other hand, the work of Cozzi and Siegel[24,26] yields a

qualitatively different trend, exhibiting excellent correlation with σ_p but no correlation with σ_m.

One potential reason for the differences between the present experimental results and previous work is that the reactions in Scheme 1 probe substituent effects in the sandwich dimer, whereas the probes mentioned above involve parallel displaced arrangements. π-Polarization effects could very well play a significant role in substituent effects in parallel displaced stacking interactions. That the present experiments probed a different dimer configuration is also one potential reason the substituent effects in the present work are significantly larger than those observed in the experiments of Gung et al.[30] and Hunter and co-workers.[33]

Conclusions

The stereoselective Diels−Alder reactions depicted in Scheme 1 have been examined experimentally and using the B3LYP, M05-2X, and M06-2X DFT functionals. Predicted solvent-corrected relative free energy barriers are in modest agreement with experimental results. Computed gas-phase relative enthalpy barriers provide much better agreement with experiment, though the M05-2X and M06-2X barriers systematically overestimate the experimental free energy differences. The deviations of the M05-2X and M06-2X results from the experimental values are attributed to dispersion effects operative in the gas-phase computations but masked by solvent interactions in the experiment.

The stereoselectivities were shown to arise primarily from differential π-stacking interactions in the competing transition states. With the exception of the dimethyl case, all reactions favor the product featuring cofacial interactions between the incoming anthracene and the more heavily substituted benzene ring of the substrate. In particular, OMe, despite being a π-electron donor, enhances the interaction in aryl−aryl sandwich complexes.

The stereoselective Diels−Alder reactions depicted in Scheme 1 provide a sensitive experimental probe of substituent effects in aryl−aryl sandwich complexes, and the present results support a model of substituent effects in the sandwich configuration of the benzene dimer advanced by Wheeler and Houk.[21,22] In this model, the π-system of the substituted benzene is unimportant and substituent effects in the sandwich dimer are governed by direct interactions between the substituent and the unsubstituted aryl ring. These substituent effects correlate with σ_m, not σ_p, indicative of the dependence on inductive/field effects rather than π-polarization.

The present experimental results provide the first clear demonstration that a π-donating but σ-withdrawing substituent stabilizes π-stacking interactions in aryl−aryl sandwich complexes. This raises doubts about the popular π-polarization-based models of these stacking interactions.[2,24–27] Instead, the present results are most readily explained by a new model (see Figure 2) in which direct interactions between the substituent and the less substituted ring dominate substituent effects in the sandwich configuration of the benzene dimer. Previous experimental results of Gung et al.[30] and Hunter and co-workers[33] are also consistent with this new model.

Acknowledgment. This work was supported by NIH-1F32GM082114 (S.E.W.) and NIH-GM36700 (K.N.H.) and in part by the National Science Foundation (MIT). A.J.M. thanks L'Oreal USA Fellowships for Women in Science for a postdoctoral fellowship. Computer time was provided in part by the UCLA Institute for Digital Research and Education (IDRE) and the National Center for Supercomputer Applications (NCSA). Figures 1, 3, and 4 were generated using CYLview.[59]

Supporting Information Available: Materials; general experimental details; general procedure for the Diels−Alder reaction; product ratios and isolated yields; synthetic procedures; NMR spectra; X-ray crystal structures and summary of bond distances; complete citations for refs 44 and 48; barrier heights for maleic anhydride + benzene; gas-phase energy barriers and free energy barriers; inter-ring distances in **TS2** and **TS3**; energy barriers for butadiene + substrates **1a**−**1e**; absolute energies, enthalpies, and free energies; optimized Cartesian coordinates. This material is available free of charge via the Internet at http://pubs.acs.org.

JA903653J

(59) Legault, C. Y. *CYLview, 1.0b*; Université de Sherbrooke: Sherbrooke, Canada, 2009; http://www.cylview.org.